


# Optimization-Free Filter and Matched-Filter Design through Spatial and Temporal Soft Switching of the Dielectric Constant

Ohad Silbiger and Yakir Hadad<sup>✉\*</sup>

*School of Electrical Engineering, Tel-Aviv University, Ramat-Aviv, Tel-Aviv 69978, Israel*

 (Received 25 May 2022; revised 9 November 2022; accepted 6 December 2022; published 18 January 2023)

The problem of inverse design is rooted to the classical problem of inverse scattering. In general, these highly nonlinear and often ill-posed problems are solved via extensive optimization techniques. In this paper, we suggest an optimization-free method for the inverse design of a one-dimensional medium with spatially inhomogeneous dielectric constant  $\epsilon(z)$ . In addition, we derive the governing equation of an analog problem—a time-dependent homogeneous medium—and use the same technique for inverse design of the temporal profile  $\epsilon(t)$  of a spatially homogeneous medium that is required to achieve a desired frequency response in  $k$ -space. Lastly, we use this optimization-free inversion approach to demonstrate the design of the reflection response such that the reflected wave undergoes a desired filtering, such as of Tchebychev type, differentiator, and a matched filter for chirp signal detection over additive Gaussian noise, which is of high potential significance in chirp radar and sonar applications.

DOI: [10.1103/PhysRevApplied.19.014047](https://doi.org/10.1103/PhysRevApplied.19.014047)

## I. INTRODUCTION

The behavior of electromagnetic waves in spatially [1,2] and temporally [3–5] varying media has been studied for a long time. Specifically, the propagation of waves in a homogeneous time-dependent medium shares similarities with steady-state wave propagation in inhomogeneous media, and has attracted a lot of interest in recent years, due to the added degree of freedom that the time variation allows. Time-dependent metamaterials have been reported to give rise to unique wave phenomena, such as nonreciprocal wave transfer [6–8], temporal photonic crystals [9,10], wideband impedance matching [11], electromagnetic isolators [12,13], unitary energy transfer [14], and exotic wave reflection phenomena [15,16]. In many cases, however, it is of interest to solve the inverse problem. For example, if the material's properties are unknown, or if specific behavior of the waves is desired. Previous studies addressed the inverse scattering problem in space, i.e., in the presence of spatial inhomogeneities, and used frequency-domain or time-domain reflection information to reconstruct the profile. For one-dimensional inversion problems, this has been done through iterative methods [17,18] or mathematical approximations of the local reflection coefficient [19,20].

In contrast, in this paper we suggest a direct, optimization-free technique that is based simply on an inverse Fourier transform over an algebraic manipulation of the local reflection coefficient, to reconstruct the dielectric profile of a one-dimensional material from the

reflection coefficient spectrum. Furthermore, we derive an analog model of a *spatially homogeneous but temporally varying medium* that shows very similar behavior, and use essentially the same approach to reconstruct the temporal profile from  $k$ -space measurements of the reflection. Lastly, we show how each of these models can be used to design a desired frequency response. The temporal switching adds a degree of freedom that together with spatial nonhomogeneity can allow high flexibility for the design of analog computing devices. As an example we design a few analog filters, including a matched filter for chirp signal detection over noise, which is common in radar applications due to its sharp response.

## II. THEORY

### A. Reflection in a one-dimensional spatially inhomogeneous medium

When an electromagnetic wave travels in a medium with spatially varying dielectric and magnetic properties, the inhomogeneity will cause reflections. For example, a time-harmonic transverse electromagnetic (TEM) wave that is propagating in a tapered transmission line along the  $z$  axis will be comprised of a superposition of forward- and backward-propagating waves [see Fig. 1(a)]. The total voltage on the line can be represented using the local reflection coefficient  $\Gamma(z)$ :

$$V(z) = V^+(z)e^{j(\omega t - \beta(z)z)} [1 + \Gamma(z)]. \quad (1)$$

\*hadady@eng.tau.ac.il

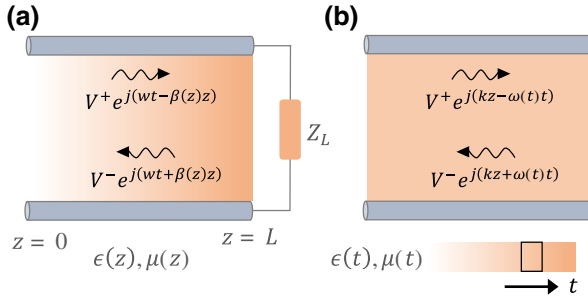


FIG. 1. (a) A transmission line with an inhomogeneous dielectric profile will support forward-traveling and backward-traveling time-harmonic waves. (b) A transmission line with a spatially homogeneous but time-varying dielectric and/or magnetic profile will support forward-traveling and backward-traveling *space-harmonic* waves.

The local reflection coefficient  $\Gamma(z)$  is subject to Riccati's equation [1]:

$$\frac{d\Gamma}{dz} = 2j\beta\Gamma - \frac{1}{2}(1 - \Gamma^2) \frac{d(\ln Z)}{dz}, \quad (2)$$

where  $\beta$  is the propagation constant in the transmission line,  $\beta(z) = \omega\sqrt{\mu(z)\epsilon(z)}$ , and  $Z$  is its characteristic impedance:  $Z(z) = \sqrt{\mu(z)/\epsilon(z)}$ . Note that this equation is valid under any continuous variation in the material's permittivity or permeability.

### B. Reflection in a temporally varying spatially homogeneous medium

Riccati's equation, Eq. (2), governs the reflection coefficient of a time-harmonic TEM wave in an inhomogeneous medium. In this section we derive the governing equation for an analog problem—a *space-harmonic* TEM wave in a time-varying and spatially homogeneous medium. Again, we resort back to the convenient transmission-line model. Consider a TEM wave propagating in an infinite transmission line containing a homogeneous medium with permittivity  $\epsilon_1$  and permeability  $\mu_1$ :

$$V = V_1 e^{j(kz - \omega t)}, \quad I = \frac{V_1}{Z_1} e^{j(kz - \omega t)}. \quad (3)$$

At time  $t$  the parameters of the line are switched to  $\epsilon_2$  and  $\mu_2$ . This changes the phase velocity of the wave from  $c_1$  to  $c_2$ , and the characteristic impedance of the line from  $Z_1$  to  $Z_2$ . The continuity of the electric displacement field  $\mathbf{D} = \epsilon_i \mathbf{E}_i$  and the magnetic field  $\mathbf{B} = \mu_i \mathbf{H}_i$  before and after switching ( $i = 1, 2$ ) renders the appearance of a reflected wave, with reflection and transmission coefficients [11]:

$$\Gamma_s = \frac{1}{2} \left( \frac{c_2}{c_1} \right) \left( \frac{Z_2}{Z_1} + 1 \right), \quad T_s = \frac{1}{2} \left( \frac{c_2}{c_1} \right) \left( \frac{Z_2}{Z_1} - 1 \right). \quad (4)$$

For the reflection and transmission dynamics under soft temporal switching, the reader is encouraged to refer to Ref. [21], and also to Ref. [22] that presents analogous results. In a transmission line with a homogeneous medium that changes with respect to time [see Fig. 1(b)], we can express the voltage at time point  $i$  as  $V_i = V_{0i} e^{j(kz - \omega_i t)}$ , which is convenient to represent using the voltage *space* phasor:

$$V(z, t) = \text{Re} \{ V(t) e^{jkz} \}, \quad (5)$$

where  $V(t)$  is a superposition of transmitted and reflected waves:

$$V(t) = V^+(t) + V^-(t) = V_0^+ e^{-j\omega(t)t} + V_0^- e^{j\omega(t)t}. \quad (6)$$

Thus we define the time-dependent reflection coefficient:

$$\Gamma(t) = \frac{V^-(t)}{V^+(t)}. \quad (7)$$

Upon a small change in the medium parameters, we may apply symmetry considerations and the superposition principle to obtain after switching

$$V(t + dt) = [T_s V_0^+ + \Gamma_s V_0^-] e^{-j\omega(t)t} + [T_s V_0^- + \Gamma_s V_0^+] e^{j\omega(t)t}. \quad (8)$$

From this equation we can express the change in  $\Gamma$  over a short time interval  $dt$ :

$$\Gamma(t + dt) = \frac{\Gamma_s + \Gamma(t) T_s}{T_s + \Gamma(t) \Gamma_s} e^{2j\omega(t)dt}, \quad (9)$$

and moreover,

$$e^{2j\omega dt} \approx 1 + 2j\omega dt. \quad (10)$$

Assuming the change in parameters is small, the temporal reflection will be much weaker than the transmission,  $T_s \gg \Gamma_s$ . Thus,

$$\frac{1}{T_s + \Gamma(t) \Gamma_s} \approx \frac{1}{T_s} \left( 1 - \Gamma(t) \frac{\Gamma_s}{T_s} \right). \quad (11)$$

Substituting in Eq. (9) and neglecting second order terms:

$$\Gamma(t + dt) = \frac{\Gamma_s}{T_s} + \Gamma(t) - \Gamma^2(t) \frac{\Gamma_s}{T_s} + 2j\omega \Gamma(t) dt. \quad (12)$$

Next, upon a small change in the characteristic impedance of the line, we obtain from Eq. (4) that

$$\frac{\Gamma_s}{T_s} = \frac{1}{2} d \ln(Z). \quad (13)$$

And, finally obtaining

$$\frac{d\Gamma}{dt} = 2j\omega\Gamma + \frac{1}{2}(1 - \Gamma^2)\frac{d(\ln Z)}{dt}. \quad (14)$$

Equation (14) is essentially identical in its form to Eq. (2). Thus, the behavior of the time-dependent reflection coefficient in a spatially homogeneous medium that undergoes temporal variation is very similar to the behavior of the space-dependent time-harmonic reflection coefficient in a spatially inhomogeneous medium. That being said, an important difference is in the definition of the reflection coefficient itself, which is related to the causality of the problems. In the spatially inhomogeneous problem, the reflection is defined with respect to the impinging wave, while in the temporally inhomogeneous one the reflection is defined with respect to the transmitted wave during the temporal switching time interval. In the following, we use approximations of the governing Eqs. (2) and (14) to reconstruct a dielectric profile (spatial or temporal) from the reflection spectrum and design desired frequency responses.

### C. Spatial profile reconstruction

Let us assume a transmission line defined between  $z = 0$  and  $z = L$ , connected to a load impedance. The normalized characteristic impedance of the line  $Z$  and the propagation constant  $\beta$  are both functions of space:  $Z = Z(z)$ ,  $\beta = \beta(z)$ . Riccati's Eq. (2) that governs the reflection coefficient along the line has no known analytical solution in its general form. However, assuming small spatial variations along the line we may assume a small reflection coefficient ( $|\Gamma|^2 \ll 1$ ), obtaining the approximated equation for  $\Gamma$ :

$$\frac{d\Gamma}{dz} = 2j\beta\Gamma - \frac{1}{2}\frac{d(\ln Z)}{dz}. \quad (15)$$

This equation has a closed-form solution. Assuming the line is matched in the end, i.e.,  $Z(z = L) = Z_L$ , the reflection coefficient at the entrance  $\Gamma_i = \Gamma(z = 0)$  can be formulated according to [1]

$$\Gamma_i = \frac{1}{2} \int_0^{\theta_L} e^{-j\theta} \frac{d}{d\theta} \ln(Z) d\theta, \quad (16)$$

where

$$\theta = \int_0^z 2\beta(z)dz, \quad \theta_L = \int_0^L 2\beta(z)dz. \quad (17)$$

As observed from the last equation, the normalization of the impedance is arbitrary and does not affect the reflection coefficient. For convenience we choose to normalize by the impedance of the load so that  $Z_L = 1$ .

In the following we assume that the material inside the line is nonmagnetic with permeability  $\mu_0$  and an unknown

permittivity profile  $\epsilon(z)$ . In the following we formulate a reconstruction the unknown profile  $\epsilon(z)$  from the spectrum of the reflection coefficient at the *line input*  $\Gamma_i(\omega)$ . Using integration by parts and since  $Z|_{\theta=\theta_L} = Z_L = 1$ ,

$$\Gamma_i = \frac{1}{2} \left[ -\ln(Z_0) + j \int_0^{\theta_L} e^{-j\theta} \ln(Z) d\theta \right], \quad (18)$$

where  $Z_0$  is the normalized characteristic impedance at  $z = 0$ . We define  $\tau = \omega^{-1}\theta$ , and through change of variables

$$\Gamma_i(\omega) = \frac{1}{2} \left[ -\ln(Z_0) + j\omega \int_0^{\tau_L} e^{-j\omega\tau} \ln(Z) d\tau \right], \quad (19)$$

where  $\tau_L = 2c_0^{-1} \int_0^L n^{-1}(z')dz'$  is the accumulated time delay for propagation along the line in the WKB approximation,  $c_0$  is the speed of light in vacuum, and  $n$  is the refractive index,  $n = \sqrt{\epsilon_r}$ .

We note that the integral on the right-hand side of Eq. (19) is the Fourier transform in the variable  $\tau$  of the natural logarithm of the characteristic impedance multiplied by a window function. Also, in light of Eq. (19), obviously  $\Gamma_i(0) = -\frac{1}{2} \ln(Z_0)$ . Therefore, some rearrangement renders

$$\frac{2[\Gamma_i(\omega) - \Gamma_i(0)]}{j\omega} = \int_0^{\tau_L} e^{-j\omega\tau} \ln(Z) d\tau. \quad (20)$$

Equation (20) shows that we can obtain the dielectric profile of the line from the spectrum of  $\Gamma_i$  by simply using the inverse Fourier transform on its left-hand side. This profile, however, is known in terms of  $\tau$ , so  $\epsilon(z)$  should be estimated from  $\epsilon(\tau)$ . For that we use

$$dz = (2c_0n)^{-1}d\tau. \quad (21)$$

Note that  $z = 0$  corresponds to  $\tau = 0$ , and thus we construct the  $z$  axis using this differential relationship until  $Z = L$ .

### D. Temporal profile reconstruction

Now let us consider a dual problem. We consider an infinite transmission line filled with homogeneous medium with permittivity and permeability  $\epsilon$  and  $\mu$ . At time  $t = 0$ , we start changing the parameters of the medium, and at time  $t = T$  the variation stops. We assume that the material has only dielectric properties; thus  $\epsilon = \epsilon(t)$ ,  $0 < t < T$ ,  $\mu = \mu_0$ . As before, for slow changes, we assume  $|\Gamma|^2 \ll 1$  and approximate the exact differential equation that governs the reflection coefficient [Eq. (14)] according to

$$\frac{d\Gamma}{dt} = 2j\omega\Gamma + \frac{1}{2}\frac{d(\ln Z)}{dt}. \quad (22)$$

Here the impedance is normalized by the impedance at time  $t = 0$ . We may follow the same process as before,

while defining  $\xi = 2c_0 \int_0^t n(t') dt'$  and  $\xi_T = 2c_0 \int_0^T n(t') dt'$ , and obtain for  $\Gamma$  at time  $T$ :

$$\frac{2[\Gamma_T(k) - \Gamma_T(0)]}{jk} = \int_0^{\xi_T} e^{-jk(\xi - \xi_T)} \ln(Z) d\xi. \quad (23)$$

See also Ref. [23]. The frequency shift here arises from the initial condition, i.e., assuming  $\Gamma(t = 0) = 0$ , meaning there is only a forward-propagating wave at  $t = 0$ . Similarly to Eq. (20), which can be used to estimate the spatial profile  $\epsilon(z)$  from the spectrum of the reflection coefficient at the entrance  $\Gamma_i(\omega)$ , Eq. (23) can be used to estimate the temporal profile  $\epsilon(t)$  from the  $k$ -space measurements of the reflection coefficient at time  $T$ ,  $\Gamma_T(k)$ .

### III. TEMPORAL AND SPATIAL FILTER INVERSE DESIGN

Equations (20) and (23) allow us to reconstruct the dielectric profile in space (time) from the *measurements* of the temporal (spatial) reflection spectrum  $\Gamma(\omega)$  [ $\Gamma(k)$ ]. However, this ability can be also applied to *desired reflection coefficients*  $\Gamma$  that we synthesize artificially in order to get a particular spatial or temporal functionality, such as band-pass filter or matched filter. Obviously, not every function can be obtained using this scheme; however, this method gives a direct solution that requires no optimization process on the selection of the profile, and thus provides a significant advantage in that respect over optimization-based techniques that are often computationally demanding. In the following, we demonstrate how the theory outlined above can be used to construct several temporal and spatial analog filters. In the following, several examples are discussed: Tchebychev low-pass filter of orders 3

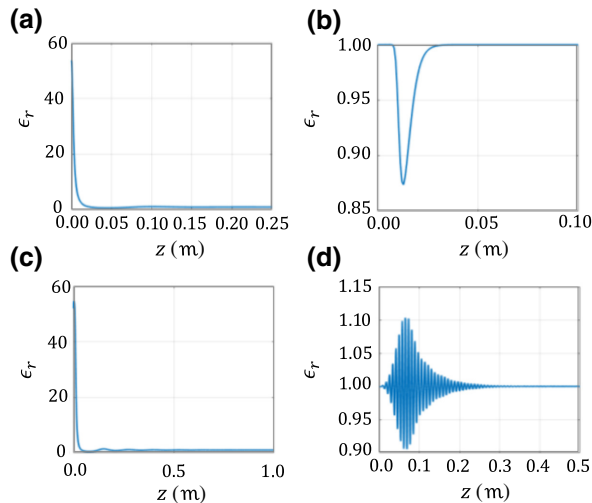


FIG. 2. Spatial profiles of the dielectric constant  $\epsilon_r(z)$  designed to formulate desired frequency responses: (a) low-pass Chebyshev filter (order 3); (b) temporal differentiator; (c) low-pass Chebyshev filter (order 8); (d) band-pass filter.

and 8, differentiator, and band-pass filter (see Figs. 2 and 4). We conclude with the design of a matched filter for chirp signal that is commonly used in radar applications [24].

The design process is as follows. For a spatially inhomogeneous transmission line, the left-hand side of Eq. (20) is calculated from the *desired* frequency response  $\Gamma(\omega)$  to give  $\ln[Z(\xi)]$ . The impedance profile is then inverted, and Eq. (21) is used to reconstruct the profile  $\epsilon(z)$ . It should be noted that Eq. (20) assumes an approximate solution of  $\Gamma$ , and, therefore, the exact reflection coefficient obtained from the reconstructed profile  $\epsilon(z)$  will be slightly different from the desired reflection spectrum  $\Gamma(\omega)$  that is fed into Eq. (20).

Figure 3 shows the reflected fields obtained after a TEM wave propagates through a number of filters, generated by the dielectric spatial profiles in Fig 2. The incident field is a Gaussian pulse (black), and its width is different for each case, to contain the frequencies affected by each filter. The reflected field at the line entrance is calculated using two methods: (1; blue) finite-difference time-domain (FDTD) simulation of the fields in the line and (2; orange) Runge-Kutta numerical calculation of the reflection coefficient  $\Gamma(\omega)$  according to Eq. (14). The latter method gives the *exact* reflection coefficient, so the predicted spectrum of the reflection coefficient is slightly different from the desired frequency responses that are fed into Eq. (20) to obtain the profiles. The spectrum of the reflected field is then calculated according to  $E^r(\omega) = \Gamma(\omega)E^i(\omega)$ , and the temporal profile of the field,  $E^r(t)$ , is calculated using the inverse Fourier transform. Figure 3 shows good agreement of the reflected signal with both methods, suggesting that the frequency response can be tailored with high precision. As the reflections in these examples are small ( $|\Gamma| \ll 1$ ), the amplitudes of the electric fields are normalized.

To obtain a desired *spatial* reflection spectrum, the process outlined above is repeated using Eq. (23). In the spatially nonhomogeneous medium, at the entrance to the line,  $E^t = E^i$ , and therefore  $\Gamma = E^t/E^i = E^r/E^i$ . In this case, however, this relationship is true only for time  $t = 0$  (and not  $t = T$ ), so we may relate the reflection coefficient only to the transmitted field. However, in a regime of slow and continuous temporal changes, we may assume the reflection is weak compared with the transmission, and with good approximation:  $\Gamma(t) \approx E^r(t)/E^i(t)$ . Figure 5 shows the spatial profile of the reflected electric fields generated by the temporal switching profiles in Fig. 4. Here we use  $E^r(k) = \Gamma(k)E^i(k)$  before using the inverse Fourier transform to obtain  $E^r(t)$ . In this case as well, the FDTD simulation is in good agreement with the results obtained from the calculation of the reflection spectrum with Eq. (14).

As a last example, in the following we design using the suggested optimization-free approach a matched filter for

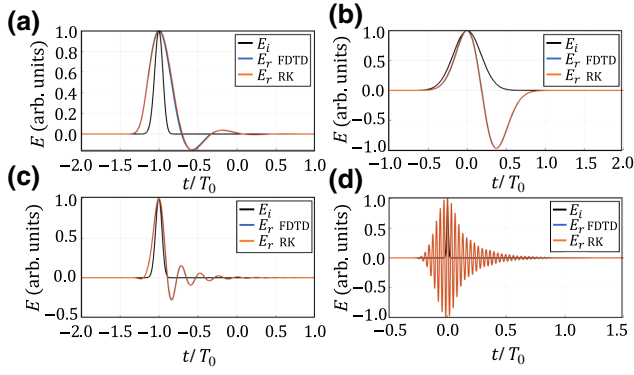


FIG. 3. Simulation results of a TEM field propagating through a nonhomogeneous medium—here only the electric field is shown. The results in (a)–(d) correspond to the spatial dielectric profiles in Fig. 2: (a) low-pass Chebyshev filter (order 3); (b) temporal differentiator; (c) low-pass Chebyshev filter (order 8); (d) band-pass filter. The time axis is normalized by  $T_0 = L/c_0$ , where  $c_0$  is the speed of light in vacuum.

chirp signal. Given an input electric field signal on the line  $E^i(z)$ , we are interested that the reflected signal will be shaped as the autocorrelation of the input, or in other words, the reflected signal should be convoluted with itself after space reversal:

$$E^r(z) = E^i(z) * E^i(-z), \quad (24)$$

where  $*$  denotes spatial convolution. In the spatial frequency domain, this is equivalent to

$$E^r(k) = E^i(k)E^i(k)^*. \quad (25)$$

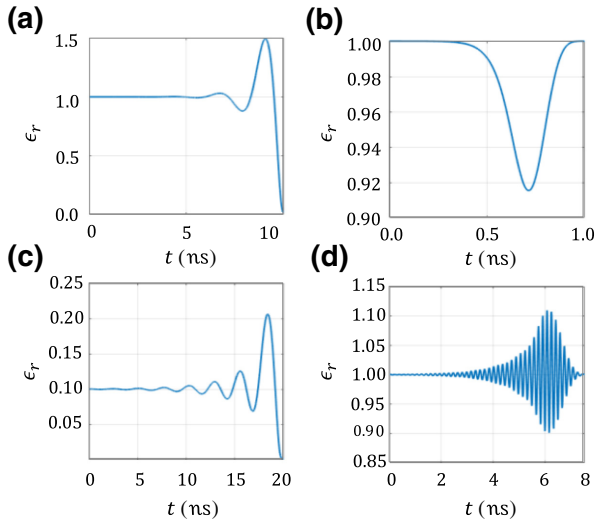


FIG. 4. Temporal profiles of the dielectric constant  $\epsilon_r(t)$  designed to formulate desired spatial frequency responses: (a) low-pass Chebyshev filter (order 3); (b) temporal differentiator; (c) low-pass Chebyshev filter (order 8); (d) band-pass filter.

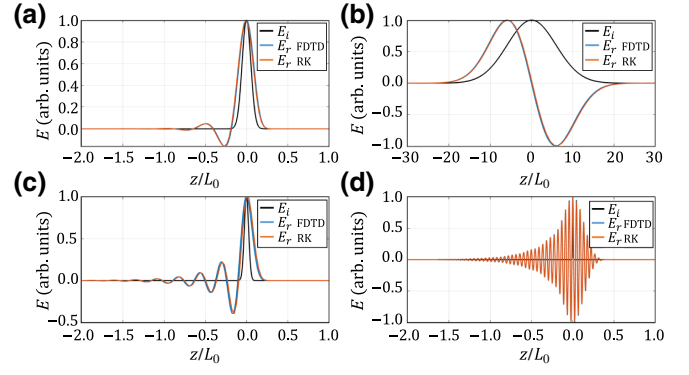


FIG. 5. Simulation results of a TEM field propagating through a homogeneous medium with temporal switching—here only the electric field is shown. The results in (a)–(d) correspond to the temporal dielectric profiles in Fig. 4: (a) low-pass Chebyshev filter (order 3); (b) temporal differentiator; (c) low-pass Chebyshev filter (order 8); (d) band-pass filter. The  $z$  axis is normalized by  $L_0 = c_0T$ , where  $c_0$  is the speed of light in vacuum.

Thus, we require that

$$\Gamma(k) = E^i(k)^*. \quad (26)$$

We use this as an input to Eq. (23) and perform the detailed algorithm discussed above to construct the required temporal switching profile of the dielectric constant. To demonstrate this, we calculate the required temporal profile for a chirp pulse:

$$E^i(z) = \sin(k^2 z^2), \quad (27)$$

where  $k = 2(1/m)$  in this example. Figure 6 shows a comparison between the theoretically required output calculated by autocorrelation of the chirp signal in Eq. (27),

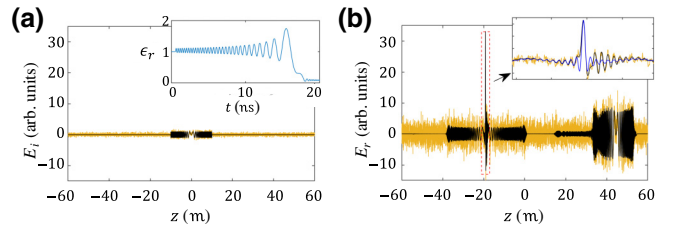


FIG. 6. Synthesis of a matched filter for chirp signal. (a) The incoming chirp signal without noise (black line) and with additive Gaussian noise (yellow line), SNR = 10. In the inset is shown the temporal profile of the dielectric constant that is required to implement this specific filter. (b) The total field after the temporal profile is activated, calculated by brute-force FDTD simulation. Again, the noiseless case is shown in black, with the noisy case in yellow. Note the reflected wave to which the manipulation has been designed. In the inset a comparison between the noisy case, noiseless case, and ideal autocorrelation (blue line) is shown, indicating an excellent agreement in the sharp peak that is expected for this signal type.

and the actual reflection that is obtained by a full-wave FDTD simulation for the designed  $\epsilon(t)$  profile and with the impinging chirp signal. To strengthen this example further, we consider the case of detection of a noisy chirp signal. Specifically, we introduce additive Gaussian noise with  $\text{SNR} = 10$ . In this case, the output signal after the matched filter provides a much clearer signature of the signal with respect to the output signal with noise. Interestingly, this matched filter is not fixed but it is inherently tunable. Fast rate temporal variations are challenging in rf and surely in optical frequencies; however, in acoustics due to the relatively low frequencies that are used, electronic manipulation of acoustic metamaterials for matched filter detection seems quite plausible with various important applications in sonar systems.

#### IV. CONCLUSIONS

In this paper, we show the similarity of the scattering problem between a temporally steady-state inhomogeneous material and a homogeneous time-dependent material. In both cases, the reflection coefficient is governed by Riccati's equation, and in both cases its approximated linearization allows a direct solution of the inverse scattering problem for a varying dielectric constant. We also show how solving the inverse scattering problem allows the inverse design of a wide range of desired frequency responses in time (through spatial inhomogeneities) and space (through temporal variation). This optimization-free technique can be used as a direct method for the design of various analog devices. In particular, we emphasize its potential in the design and implementation of tunable analog matched filters, with important applications in radar and sonar systems.

#### ACKNOWLEDGMENTS

This research is supported by the Israel Science Foundation (Grant No. 1353/19).

---

[1] R. E. Collin, *Foundations for Microwave Engineering* (New Jersey, Wiley and Sons, 2001), 2nd ed.  
 [2] L. R. Walker and N. Wax, Non-uniform transmission lines and reflection coefficients, *J. Appl. Phys.* **17**, 1043 (1946).  
 [3] F. R. Morgenthaler, Velocity modulation of electromagnetic waves, *IEEE Trans. Microw. Theory Tech.* **6**, 167 (1958).  
 [4] L. Felsen and G. Whitman, Wave propagation in time-varying media, *IEEE Trans. Antennas Propag.* **18**, 242 (1970).  
 [5] R. Fante, Transmission of electromagnetic waves into time-varying media, *IEEE Trans. Antennas Propag.* **19**, 417 (1971).  
 [6] A. Shaltout, A. Kildishev, and V. Shalaev, Time-varying metasurfaces and Lorentz non-reciprocity, *Opt. Mater. Express* **5**, 2459 (2015).

[7] Y. Hadad, J. Soric, and A. Alú, Breaking temporal symmetries for emission and absorption, *PNAS* **113**, 3471 (2016).  
 [8] D. L. Sounas and A. Alú, Non-reciprocal photonics based on time modulation, *Nat. Photonics* **11**, 774 (2017).  
 [9] J. R. Zurita-Sánchez, P. Halevi, and J. C. Cervantes-González, Reflection and transmission of a wave incident on a slab with a time-periodic dielectric function  $\epsilon(t)$ , *Phys. Rev. A* **79**, 053821 (2009).  
 [10] J. S. Martínez-Romero, O. M. Becerra-Fuentes, and P. Halevi, Temporal photonic crystals with modulations of both permittivity and permeability, *Phys. Rev. A* **93**, 063813 (2016).  
 [11] A. Shlivinski and Y. Hadad, Beyond the Bode-Fano Bound: Wideband Impedance Matching for Short Pulses Using Temporal Switching of Transmission-Line Parameters, *Phys. Rev. Lett.* **121**, 204301 (2018).  
 [12] S. Taravati, N. Chamanara, and C. Caloz, Nonreciprocal electromagnetic scattering from a periodically space-time modulated slab and application to a quasisonic isolator, *Phys. Rev. B* **96**, 165144 (2017).  
 [13] H. Lira, Z. Yu, S. Fan, and M. Lipson, Electrically Driven Nonreciprocity Induced by Interband Photonic Transition on a Silicon Chip, *Phys. Rev. Lett.* **109**, 033901 (2012).  
 [14] Y. Mazor, M. Cotrufo, and A. Alú, Unitary Excitation Transfer between Coupled Cavities Using Temporal Switching, *Phys. Rev. Lett.* **127**, 013902 (2021).  
 [15] V. Bacot, M. Labousse, A. Eddi, M. Fink, and E. Fort, Time reversal and holography with spacetime transformations, *Nat. Phys.* **12**, 972 (2016).  
 [16] V. Pacheco-Peña and N. Engheta, Temporal equivalent of the Brewster angle, *Phys. Rev. B* **104**, 214308 (2021).  
 [17] A. G. Tijhuis and C. Van der Worm, Iterative approach to the frequency-domain solution of the inverse-scattering problem for an inhomogeneous lossless dielectric slab, *IEEE Trans. Antennas Propag.* **32**, 711 (1984).  
 [18] Y. M. Wang and W. C. Chew, An iterative solution of the two-dimensional electromagnetic inverse scattering problem, *Int. J. Imaging Syst. Technol.* **1**, 100 (1989).  
 [19] W. Tabbara, Reconstruction of permittivity profiles from a spectral analysis of the reflection coefficient, *IEEE Trans. Antennas Propag.* **27**, 241 (1979).  
 [20] G. Mazzarella and G. Panariello, Reconstruction of one-dimensional dielectric profiles, *J. Opt. Soc. Am.* **8**, 1622 (1991).  
 [21] Y. Hadad and A. Shlivinski, Soft temporal switching of transmission line parameters: Wave-field, energy balance, and applications, *IEEE Trans. Ant. Prop.* **68**, 1643 (2020).  
 [22] E. Galiffi, S. Yin, and A. Alú, Tapered photonic switching, *Nanophotonics* **11**, 3575 (2022).  
 [23] O. Silbiger and Y. Hadad, Optimization-Free Design of Spatial Analog Filters by Temporal Variation, "The Seventeenth International Congress on Artificial Materials for Novel Wave Phenomena – Metamaterials, (Siena, Italy, September 12-17, 2022).  
 [24] J. R. Klauder, A. C. Price, S. Darlington, and W. J. Albersheim, The theory and design of chirp radars, *Bell Syst. Tech. J.* **39**, 745 (1960).